Geochronology of the Gloserheia pegmatite, Froland, southern Norway

HALFDAN BAADSGAARD, CATHERINE CHAPLIN & WILLIAM L. GRIFFIN

Baadsgaard, H., Chaplin, C. & Griffin, W. L.: Geochronology of the Gloserheia pegmatite, Froland, southern Norway. *Norsk Geologisk Tidsskrift,* Vol. 64, pp. 111–119. Oslo 1984. ISSN 0029-196X.

Relatively unaltered feldspars from the Gloserheia pegmatite yield an Rb–Sr isochron age of 1062 ± 11 Ma(M.S.W.D. = 90, Sr_I = 0.7023 ± 0.0002) and a Pb–Pb isochron age of 1085 ±28 Ma. The best age of pegmatite crystallization is given by a U–Pb concordia-discordia intersection at 1060^{+8}_{-6} Ma from euxenite samples. The radiometric ages limit the last major metamorphism in the area to > 1060 Ma, although mild later hydration has reset Rb–Sr mineral dates on muscovite and biotite to as low as ~850 Ma. O, Sr and Pb isotope data indicate that the pegmatite magma was derived from a mantle source.

Halfdan Baadsgaard, Dept. of Geology University of Alberta, Edmonton, Canada.
Catherine Chaplin, Dept. of Geology University of Alberta, Edmonton, Canada.
William L. Griffin, Mineralogisk-Geologisk Museum, Sarsgt. 1, Oslo 5, Norway.

Complex pegmatites containing unusual minerals are recognized to possess very suitable material for radiometric dating. Pegmatitic uraninite having concordant U–Th–Pb ages was used to 'geologically' determine both the decay constant of ^{40}K (to ^{40}Ar) (Wetherill et al. 1956) and ^{87}Rb (Aldrich et al. 1956), using mica cogenetic with the uraninite. The complex pegmatite examined in this study contains biotite, muscovite, plagioclase, K-feldspar, xenotime and euxenite. Because of the very large grain size of the pegmatitic minerals, whole-rock dating is impractical and only minerals were analyzed. Of the applicable radiometric methods, Rb–Sr, U–Pb and Pb–Pb were used. These isotopic analyses were carried out with the hope of determining a time of crystallization of the pegmatite, recognizing a source for the pegmatitic magma and looking for possible isotopic variations in the zones of the pegmatite. The isotopic composition of oxygen was measured on separated minerals from several samples, to determine the extent to which meteoric waters may have affected the pegmatite after its crystallization.

Geological setting

The Gloserheia granite pegmatite is a large (800 × 150 m), complexly zoned body located ca. 9 km N. of the town of Arendal in SE Norway. (Fig. 1) It intrudes Precambrian gneisses of the Bamble formation which have been metamorphosed to upper amphibolite – intermediate-P granulite facies. Foliations in the country rocks are sharply crosscut by the pegmatite, indicating that the pegmatite is post-tectonic with regard to the last major metamorphic episode in the area. Some later disturbance is, however, suggested by deformation of plagioclase lamellae, chloritization of biotite, and sericitization of feldspars.

The pegmatite is V-shaped in plan with a massive quartz core (Åmli 1977). The core had a volume of at least 100,000 m^3, and was mined from 1881 to 1982, mainly for use in ceramics and metallurgy. The pegmatite shows a well-developed, regular zonal structure, consisting of the following mappable divisions (Åmli 1977).

1) Core: massive quartz, locally miarolitic, very minor microcline and apatite, often in very large crystals, trace xenotime and monazite.
2) Intermediate zone I (0.5 – 3 m): coarse blocky microcline crystals, interstitial biotite and quartz, large apatite crystals.
3) Int. zone II (0.2–1 m): coarse anhedral plagioclase.
4) Int. zone III (c. 0.1 m): plagioclase, minor microcline and quartz. Local extensive secondary muscovitization, with concentrations of euxenite, allanite, apatite, zircon and uranium minerals.
5) Int. zone IV (c. 0.1 m): graphically intergrown quartz and plagioclase.
6) Int. zone V (5 – 8): graphically intergrown quartz and microcline.

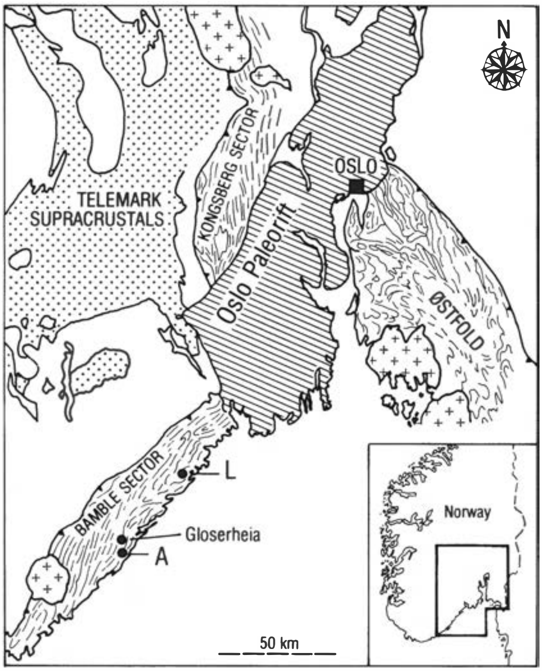

Fig. 1. Location of the Gloserheia pegmatite, A, Arendal; L, Levang gneiss dome.

7) Wall zone (0.1–1.5): quartz and plagioclase, hypidiomorphic granular microstructure.
8) Border zone ($\lesssim$ 0.1 m): similar to wall zone but finer-grained, with more biotite and magnetite.

The apatites of the core and zones I and III contain abundant inclusions of xenotime and monazite. The REE patterns of these phases suggest that the xenotime and monazite formed by exsolution from the apatite, possibly accompanied by metasomatism (Åmli 1975). All three phases show an increase in the ratio LREE/HREE toward the core, and with time within each zone, suggesting that the pegmatite crystallized inward from the walls. *Separate* crystals of xenotime from zone III, and in replacement veins through zone I, do not follow these trends. They appear to have formed late in the pegmatite crystallization history, together with euxenite and allanite (Åmli 1975).

The oldest rocks of the Bamble province are gneisses, dated to 1400–1600 Ma by Rb–Sr whole-rock methods and by U–Pb analyses of zircon (O'Nions & Baadsgaard 1971, Field & Råheim 1979). There is also abundant geochronological evidence for a thermal event in the 1000–1200 Ma period. U–Pb analyses of zircons from the reactivated portion of Levang gneiss dome (ca. 25 km NE of Gloserheia), give upper-intercept dates of ca. 1060 Ma, identical to concordant dates on sphene. Similar U–Pb dates are obtained on zircon and allanite from syn- and post-metamorphic pegmatites in the same area (O'Nions & Baadsgaard 1971). K–Ar analyses of amphiboles from the Levang area suggest a thermal peak at c. 1100 Ma, cooling over c. 120 Ma (O'Nions et al. 1969). K–Ar dates on biotite from several pegmatites and granites from Bamble cluster in the period 830–900 Ma (Broch 1964). Rb–Sr mineral isochrons on several granulites from the Arendal area record ages of c. 1040 Ma (Field & Råheim 1979). The Bamble region, and the related Kongsberg sector to the north, are intruded by numerous post-tectonic granites that yield Rb–Sr whole-rock isochron ages of 900–1000 Ma (Killeen & Heier 1975, Pedersen et al. 1978). Many of these, especially the youngest ones, have low values of I_{Sr}, suggesting that they are dominantly of juvenile origin.

There has been considerable discussion about the interpretation of the 1000–1200 Ma radiometric dates. These dates have been widely accepted as giving the age of the last regional high-grade metamorphic event, which has thus been correlated with the Grenville episode of eastern North America (Torske 1977, Falkum & Pedersen 1980). The rejuvenation of the Levang gneiss dome has been correlated with this event (O'Nions & Baadsgard 1971). Jacobsen & Heier (1978) demonstrated that syntectonic granites in the Kongsberg sector gave Rb–Sr whole rock ages of 1050–1200 Ma, and were derived from older (ca. 1600 Ma) crustal material.

Field & Råheim (1979), on the other hand, argue that the 1000–1200 Ma ages reflect only minor alteration of much older metamorphic rocks, and relate this alteration to the discoloration of granulites. Smalley et al. (1983) show that there is no clear relationship of Rb–Sr resetting to color, and conclude that the resetting is caused by minor pegmatite intrusions. Smalley et al. obtained a whole-rock Rb–Sr date of ca. 1200 Ma on an intrusive body (the Gjerstad augen gneiss). They interpret this as an intrusion age, and a minimum age for the last metamorphic event. This interpretation may be questioned, however, since the body in question is itself intensely deformed and recrystallized.

In summary: available geochronological data from the Bamble sector demonstrate that older gneisses (ca. 1400–1600 Ma) were affected by a thermal episode ca. 1000–1200 Ma ago. It is still unclear whether this episode involved high-grade tectonothermal metamorphism. If it did not, then the source of the heat is not obvious, since the major intrusion of granitic material into the terrain postdates the apparent thermal peak by 100–200 Ma. There are also possible thermal effects at 830–900 Ma when the K–Ar dates on micas were reset.

Analytical methods

Biotite, muscovite, plagioclase, K-feldspar and quartz were separated and purified by conventional magnetic and heavy-liquid techniques. Xenotime was obtained by acid leaching of the host apatite crystals, then further purified using heavy-liquids and magnetic separation. Euxenite was collected by hand picking pure chips and grains of the mineral.

Rb-Sr analysis involved HF–HNO_3 decomposition of the spiked mineral, co-precipitation of Sr with pure $Ba(NO_3)_2$, and purification of the Sr on a cation-exchange column. The Rb was separated from the supernatant liquid of the $Ba(NO_3)_2$ precipitation by addition of H_2SO_4, evaporation and ignition, leaching of alkalis with H_2O and $HClO_4$ precipitation of (K, Rb)ClO_4. U–Pb isotopic determinations on xenotime and euxenite used the Krogh (1973) method of decomposition, co-precipitation of Pb with $Ba(NO_3)_2$ and purification of the Pb on a chloride anion-exchange column. Uranium was taken from the supernatant liquid of the $Ba(NO_3)_2$ precipitation by means of a nitrate anion-exchange column. Pb separations on feldspar were carried out by HF – HNO_3 decomposition co-precipitation of the Pb with $Ba(NO_3)_2$ and chloride anion-exchange purification. All isotopic measurements of the separated elements were made on a V. G. Micromass 30 mass spectrometer, except for Rb, which was analyzed with a 12-inch solid-source instrument constructed at the University of Alberta by G. L. Cumming. Average blanks for the various procedures amount to 1.2 ng Sr, 2.6 ng Rb, <1 ng U, 1.2 ng Pb (Krogh procedure) and 3.1 ng Pb (feldspar Pb-extraction procedure). In almost all cases, the blank correction was less than one part per thousand of the analyzed constituent. (A more detailed description of the analytical methods may be found in Chaplin 1981.)

Results

Rubidium-strontium

The results of the Rb-Sr determinations are given in Table 1 and presented in a series of Figures (2–5) because of differences in scale and data distribution. The isochron diagram for biotite is given in Figure 2, for muscovite in Figure 3, for relatively unaltered K-feldspar in Figure 4, and for plagioclase in Figure 5. Comparison of Figures 2–5 shows that the four minerals yield strontium variation plots giving different approximate dates, and with the data points scattered outside the limits of analytical variation about straight lines. The variable Rb-Sr mineral results were not unexpected since petrographic examination of the minerals showed almost all plagioclase to be strongly sericitized, the biotite bent and somewhat chloritized, and the muscovite fresh and apparently unaltered. The microcline revealed replacement by sericite and quartz along small fractures in some samples, while untwinned (orthoclase?) K-feldspar in the outer zones was subject to kaolinization. The eleven relatively unaltered (petrographic examination) potassic feldspars plotted in Figure 4 give the best line (1062 ± 11 Ma), though the M.S.W.D. is still much larger than one. The initial $^{87}Sr/^{86}Sr$ ratio of 0.7023 falls in the range of values considered to be from 'mantle-derived' rocks, and the date is thought to be close to that for original crystallization of the pegmatite. If the original time of crystallization of the pegmatite minerals was $\sim$1060 Ma, then the micas (especially biotite) have lost radiogenic strontium while plagioclase has gained radiogenic strontium at some time notably later than 1060 Ma ago. This pattern of gain and loss of radiogenic strontium has been found for other minerals (see Brooks 1968) and experimentally observed as a result of secondary heating (Baadsgaard & Van Breemen 1970).

Uranium-lead

U-Pb analyses on an xenotime and several euxenite samples are given in Table 2 and plotted on a concordia diagram in Figure 6. A regression line on the euxenite samples (calculated by the method described by Ludwig (1980) gives an upper intersection with the concordia line at 1060^{+8}_{-6}

Table 1. Rb/Sr analytical data for minerals from the Gloserheia pegmatite.

Sample Number	^{86}Sr (ppm)	^{87}Rb (ppm)	$^{87}Rb/^{86}Rb$ atomic ratio	$^{87}Sr/^{86}Sr$ atomic ratio
Potassium feldspar – relatively unaltered				
C-2 *	9.4773	146.49	15.279	0.9362
CI-1 *	7.7928	122.98	15.600	0.9398
CI-4 *	7.0063	142.42	19.923	1.0021
IZ1-5 *	6.5390	143.63	21.712	1.0292
IZ1-11 *	7.4363	130.52	17.349	0.9612
IZ5-1 *	5.3369	93.329	17.286	0.9601
Plagioclase				
IZ1-4	3.0078	0.5015	0.1648	0.7223
IZ2-2	3.2183	0.2210	0.0679	0.7182
IZ2-3	2.2707	0.2478	0.1079	0.7196
IZ2-6	1.0935	0.6484	0.5862	0.7275
IZ2-7	5.7252	3.7235	0.6429	0.7185
IZ2-8	2.4478	0.7001	0.1348	0.7208
IZ3-2	6.7749	6.1227	0.8933	0.7257
IZ3-3	6.5803	4.7036	0.7066	0.7230
Feldspars. Heavier and lighter separates from perthites				
IZ1-8 +*	6.5809	13.864	2.8025	0.7435
IZ1-8 –	5.2973	3.6910	0.6887	0.7234
IZ4-1 +*	4.6603	92.343	19.587	0.9994
IZ4-1	2.8429	1.3779	0.4791	0.7208
IZ4-2 +*	4.6080	33.423	7.1667	0.8164
IZ4-2 –	3.1175	2.6887	0.8525	0.7264
IZ5-2 –*	2.2128	29.581	13.214	0.9018
IZ5-2 –*	0.2108	2.3943	11.225	0.8745
BZ-1 –	10.971	9.6044	0.8654	0.7241
Muscovite				
C-1	0.9809	121.87	122.80	2.2682
IZ1-4	0.9367	98.847	104.32	2.1772
IZ1-10	0.7529	104.34	136.99	2.6130
IZ2-1	0.8984	130.18	143.23	2.8307
IZ2-1	0.8815	130.77	146.64	2.8600
IZ2-2	1.0781	102.57	94.049	2.0042
IZ2-3	0.6547	55.734	84.146	1.9272
IZ2-6	0.7812	92.769	117.38	2.3374
IZ2-8	0.8739	104.66	118.37	2.4030
Biotite				
CI-1	0.5149	405.46	778.32	10.483
CI-2	0.3152	339.61	1253.4	18.112
IZ1-3	0.6927	448.63	640.16	8.334
IZ1-11	0.3056	442.68	1431.9	18.838
IZ2-5	0.2808	409.06	1440.2	19.460
IZ3-3	2.3003	69.439	29.841	1.0067
IZ3-3	2.1926	66.545	30.001	1.0130
IZ4-1	0.4651	454.05	965.08	13.484
IZ4-2	0.2908	496.56	1688.8	22.372

* relatively unaltered mineral sample used in the K-feldspar isochron.
\+ mineral separate with lighter specific gravity.
– mineral separate with heavier specific gravity.

Symbols: BZ, border zone; WZ, wall zone; IZ 1–5, Intermediate zones I–V (see text for relative position and mineralogical composition); CI, contact between core and intermediate zone I; C, core (large K-feldspar ×ls. in quartz core).

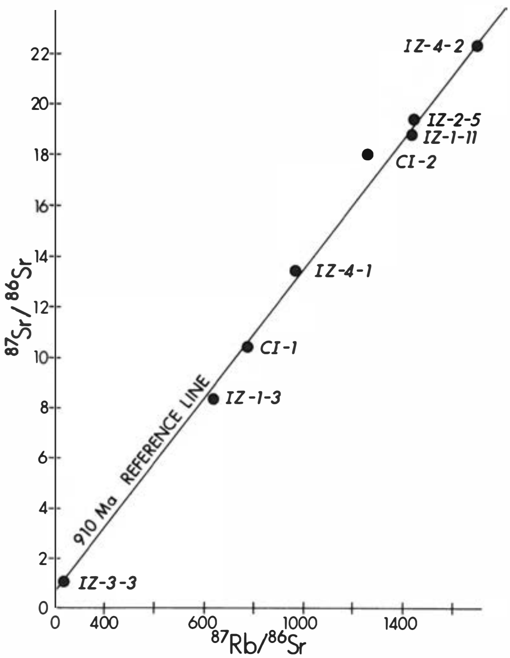

Fig. 2. Rb-Sr isochron plot of the Gloserheia biotite samples.

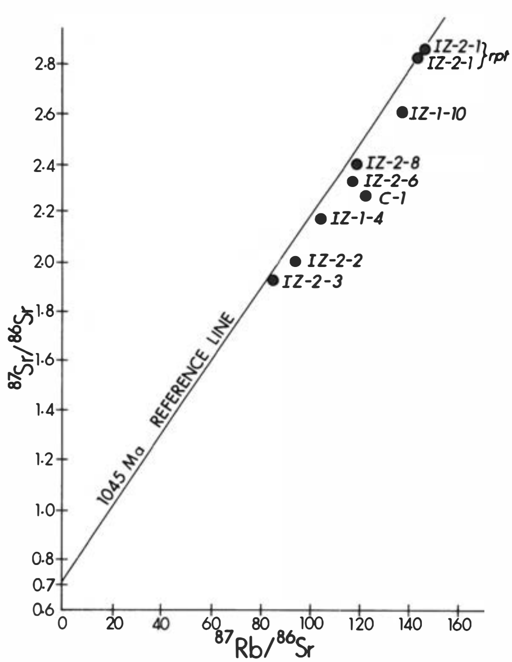

Fig. 3. Rb-Sr isochron plot of the Gloserheia muscovite samples.

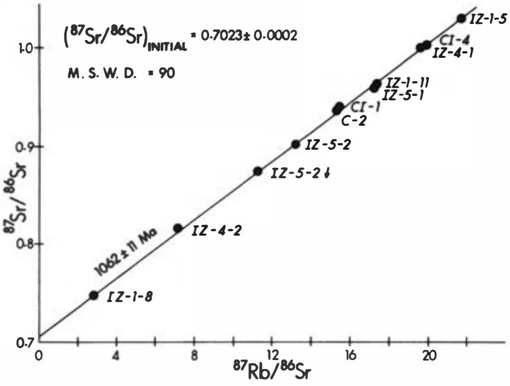

Fig. 4. Rb-Sr isochron plot of the relatively unaltered potassic feldspars from the Gloserheia pegmatite. The ± 11 Ma is an expanded error = ± 1 σ × $\sqrt{MSWD}$.

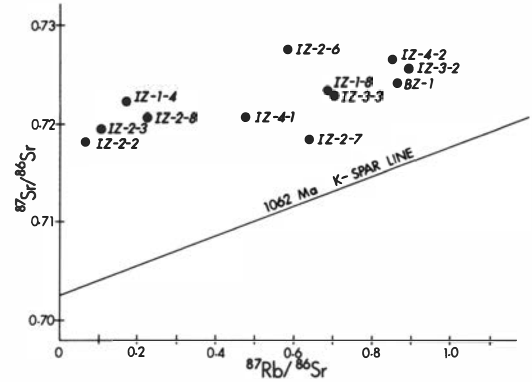

Fig. 5. Rb-Sr isochron plot of the Gloserheia plagioclase samples. All the plagioclase samples have gained radiogenic ^{87}Sr relative to the unaltered K-feldspars. This change probably occurred at the time of loss of radiogenic ^{87}Sr from the micas (~900 Ma) and likely accompanied the minor sericitization observed in the plagioclase samples.

Ma (2σ errors). The M.S.W.D. for the euxenite regression line is 35, indicating variation of data points (from a straight line) outside analytical error. The lower concordia intersection for this line is ~400 Ma, but the continuous Pb-diffusion model (Wasserburg 1963) predicts a lower intercept closer to ~100 Ma. The determined intercept could be biased towards a higher value by the apparent metamorphism (at around 900 Ma) indicated by Rb-Sr results on the biotites. The xenotime yields an essentially concordant U-Pb date of ~1030 Ma. Found as oriented filament-like crystals within large apatite crystals, the xenotime possibly formed when the apatite cooled or was subjected to metasomatism, whereby the xenotime exsolved from the apatite lattice. The 1060 Ma intersection age for the euxenite probably represents a value close to the original crystallization of the euxenite, particularly since it compares closely to the Rb-Sr isochron age of the essentially unaltered potassic feldspars.

Lead-lead

To further examine isotope variation within the pegmatite, potassic feldspars from each internal zone were analyzed for their lead isotope ratios. The results are given in Table 3 and plotted on a $^{207}Pb/^{204}Pb$ vs $^{206}Pb/^{204}Pb$ diagram in Figure 7. The plotted points scatter outside the analytical limits for a straight line, but follow a 1100-Ma-slope reference line closely. Many of the feldspar samples contain highly radiogenic lead. However, if only the less radiogenic samples are plotted (see Figure 8), they fit on a regression line within nominal analytical error (M.S.W.D.=2.39). This

Table 2. Measured Pb Isotope Ratios

Sample	$^{206}/_{204}$	$^{207}/_{206}$	$^{208}/_{206}$	^{238}U, ppm	^{206}Pb, ppm	$^{206}Pb/^{238}U$	$^{207}Pb/^{235}U$
(Xenotime)							
IZ-1-6	16949 ± 575	0.07401 ± 1	0.3660 ± 1	1151	173.4	0.1741	1.7565
Euxenites							
IZ-1-8	14493 ± 420	0.07611 ± 2	0.11232 ± 4	97554	15237	0.1805	1.8695
IZ-3-2A	11905 ± 142	0.07344 ± 1	0.11880 ± 2	86045	10878	0.1461	1.4551
IZ-3-2B	7194 ± 259	0.07433 ± 1	0.12113 ± 2	79235	10178	0.1484	1.4808
IZ-3-3	15385 ± 237	0.07545 ± 4	0.12333 ± 7	78904	11833	0.1733	1.7883
IZ-3-4	43478 ± 3800	0.07301 ± 3	0.11027 ± 4	95793	12573	0.1516	1.5197
WZ-2	8264 ± 205	0.07541 ± 1	0.08973 ± 4	105664	15571	0.1703	1.7303

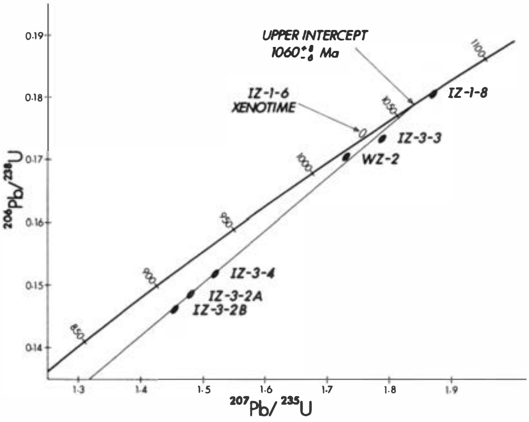

Fig. 6. Concordia plot of euxenites and one xenotime from the Gloserheia pegmatite.

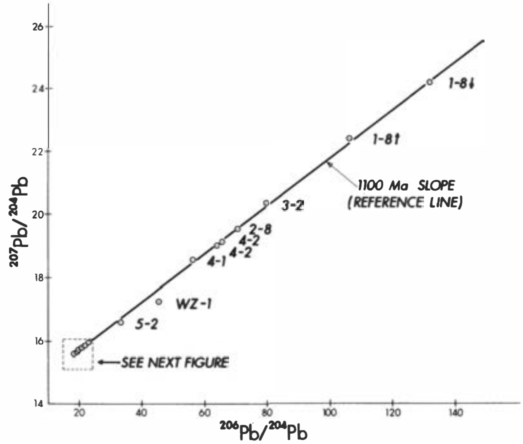

Fig. 7. Pb-Pb plot of lead isotope ratios from potassic feldspars.

line has a slope age of 1085±28 Ma, but intersects the 'mantle' lead growth curve proposed by Stacey & Kramers (1975) at about 1200 Ma. If the second stage M of Stacey and Kramers is changed from 9.74 to 9.695, the feldspar lead line becomes a single stage line.

Ludwig & Silver (1977) have shown that acid-leaching of lead from feldspar can reveal lead-isotope inhomogeneity in the mineral. Accordingly, a set of Gloserheia feldspar samples was ground to <200 mesh powder and leached with HNO_3 and dilute HF for 15 minutes. The residue from the leaching was collected, washed thoroughly with vapor-distilled H_2O and analyzed for Pb isotopes. The results are given in Table 3 and plotted in Figure 9. This plot shows the radiogenic component of the feldspar Pb to be strongly leached from the minerals. This radiogenic lead must be introduced into the K-feldspar either from uranium trapped in the feldspar at the

Table 3. Feldspar Lead Isotope Ratios – Gloserheia Pegmatite. Measured Pb Ratios

Sample	$^{207}/_{206}$	$^{208}/_{206}$	$^{204}/_{206}$	$^{206}/_{204}$	$^{207}/_{204}$	$^{208}/_{204}$
IZ-1-10↑	*0.8032 ± 2	1.9177 ± 5	0.05120 ± 6	19.53	15.69	37.39
BZ-1 ↑	*0.7949 ± 2	1.9090 ± 4	0.05062 ± 4	19.76	15.70	37.71
IZ-1-11	*0.70349 ± 4	1.7035 ± 1	0.04420 ± 1	22.62	15.92	38.54
IZ-1-4	*0.8492 ± 1	2.006 ± 1	0.05446 ± 5	18.36	15.59	36.83
CI-I	*0.76354 ± 8	1.8092 ± 5	0.04844 ± 2	20.64	15.76	37.35
IZ-2-7	*0.80792 ± 5	1.9228 ± 2	0.05156 ± 4	19.39	15.67	37.29
LEACHED	0.84006 ± 3	1.9847 ± 1	0.5385 ± 1	18.57	15.60	36.86
IZ-4-1↑	0.33079 ± 1	0.78150 ± 7	0.017843 ± 3	56.05	18.54	43.80
LEACHED	0.53406 ±	1.2626 ± 1	0.03250 ± 1	30.77	16.43	38.85
IZ-5-2↑	0.49787 ± 4	1.2096 ± 2	0.03002 ± 2	33.31	16.59	40.29
LEACHED	0.61283 ± 3	1.4757 ± 4	0.03835 ± 6	26.08	15.98	38.48
IZ-3-2	0.25558 ± 2	0.61352 ± 4	0.01256 ± 1	79.62	20.35	48.85
LEACHED	0.4238 ± 2	1.0085 ± 4	0.02454 ± 4	40.75	17.27	41.10
IZ-1-8↓	0.18341 ± 2	0.40333 ± 5	0.007582 ± 3	131.89	24.19	53.20
LEACHED	0.27917 ± 1	0.65175 ± 4	0.014289 ± 5	69.98	19.54	45.61
WZ-1	0.37948 ± 4	0.94525 ± 7	0.022002 ± 3	45.45	17.25	42.96
LEACHED	0.33401 ± 3	0.82778 ± 5	0.019758 ± 9	50.61	16.91	41.90
IZ-2-8↑	0.27720 ± 1	0.75711 ± 2	0.014198 ± 3	70.43	19.52	53.32
IZ-4-2↑	0.29739 ± 1	0.69235 ± 1	0.01565 ± 1	63.90	19.00	44.24
IZ-1-8↑	0.21121 ± 3	0.48318 ± 9	0.009424 ± 5	106.11	22.41	51.27
IZ-4-2	0.29161 ± 1	0.68172 ± 2	0.015250 ± 4	65.57	19.12	44.70
IZ-5-1	*0.72994 ± 7	1.7688 ± 8	0.04607 ± 1	21.71	15.84	38.39

* samples low in radiogenic lead used in Figure 8.

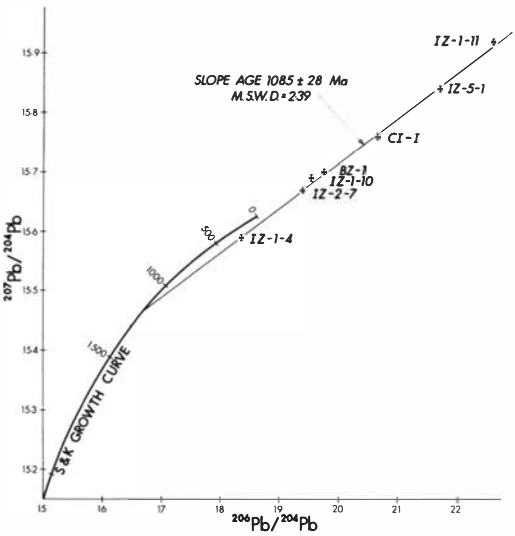

Fig. 8. Pb-Pb plot of the seven least radiogenic leads from the potassic feldspars. The S & K growth curve is that of Stacey and Kramers (1975) One sigma errors used in regression are: $^{206}/204 - 0.2‰$, $^{207}/204 - 0.25‰$, correlation coefficient p = 0.8.

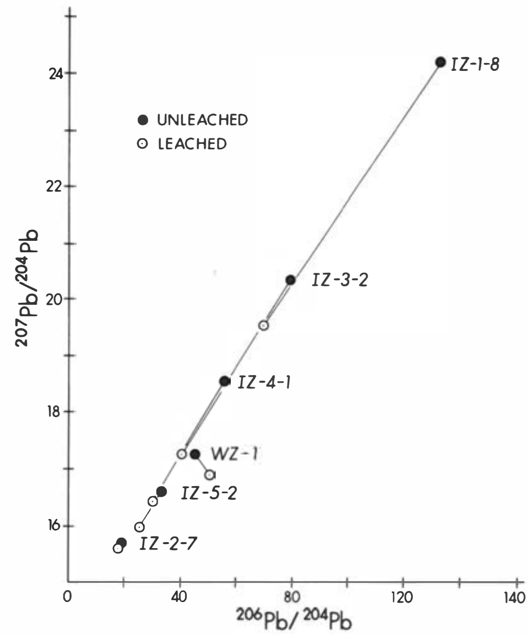

Fig. 9. Pb-Pb plot of lead isotopes from unleached versus acid-leached potassic feldspars.

time of crystallization, or during subsequent metamorphic recrystallization. Because the acid leaching did not unduly change the Pb-Pb slope age of the feldspars, it is suspected that the radiogenic lead is derived from tiny inclusions of U-rich phases enclosed in feldspar during the initial crystallization. The two initial feldspar samples with the most highly-radiogenic lead were analyzed for uranium and found to contain 40.9 ppm U (IZ-1-8) and 6.5 ppm U (IZ-3-2). The two pegmatite zones, IZ-1 and IZ-3, from which these samples were taken also contain the most abundant euxenite. Crushing and leaching the feldspar samples with acid thus removed a large portion of the uranium contaminant.

Oxygen isotopes

In order to see if oxygen isotope variation shows any correlation with the observed Sr isotope variation, samples were analyzed by the BrF_5 method of Clayton & Mayeda (1963). The data are reported with respect to SMOW (Craig 1961) in the usual $\delta^{18}O$ notation. A one-sigma standard deviation of ±0.1‰ in measured $\delta^{18}O$ was calculated from the pooled residual variance of replicate analysis of a variety of other samples analyzed in the laboratory during the period of these measurements.

Results of the oxygen isotope measurements on selected minerals from the Gloserheia pegmatite are given in Table 4 and plotted versus the pegmatite zone in Figure 10. The data show that the $\delta^{18}O$-values fall within the upper part of the range established for granitic pegmatites (Taylor & Friedrichsen 1983), and the usual igneous isotope enrichment patterns for the minerals are obtained; $\delta^{18}O$ values increase in the order biotite-muscovite-potassium feldspar-quartz. Since

Table 4.

Sample	Quartz (±0.1‰)	K-Feldspar (±0.1‰)	Biotite (±0.1‰)	Muscovite (±0.1‰)
C-1	+12.8‰			+9.3‰
C-4	+10.8‰			
C-5	+11.4‰			
C-6	+11.2‰			
C-7	+11.7‰			
CI-1	+10.6‰	+10.1‰	+7.1‰	
IZ1-2	+10.5‰			
IZ1-11	+11.9‰	+10.5‰	+7.5‰	
IZ2-1	+11.4‰			+9.7‰
IZ4-1	+11.3‰	+ 9.2‰	+5.5‰	

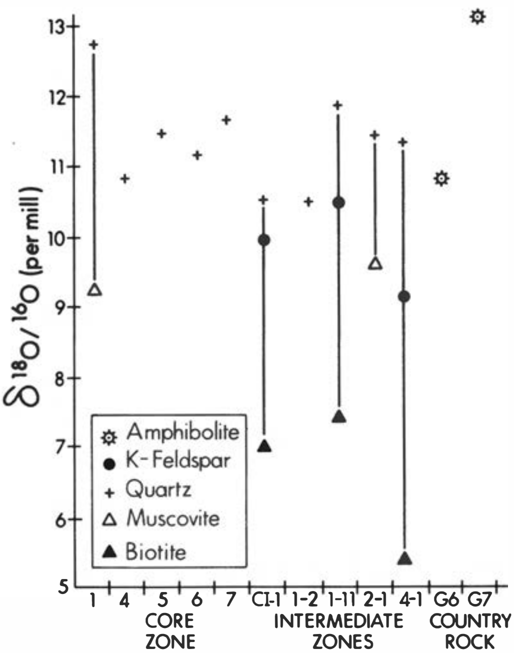

Fig. 10. Oxygen isotope values of selected minerals from the Gloserheia pegmatite.

no quartz-feldspar reversals occur, the probability of strong interaction of the pegmatite minerals with hydrothermal waters is remote. If temperatures are estimated from the quartz-mica pairs (Clayton 1981), values ranging from 600 to 300°C are obtained. This temperature variation may arise from the presence and persistence of local isotopic exchange with an aqueous vapor phase created by resurgent boiling (see Taylor & Friedrichsen 1978). Alternatively, the range of oxygen isotope mineral temperatures may be caused by a later thermal metamorphism which variably disturbed the Sr and O isotope values and induced mild sericitization of the plagioclase.

Significant alteration of the pegmatite by meteoric waters or weathering processes is precluded by the strong positive enrichment of ^{18}O in various mineral phases. The oxygen isotope data appear consistent with an igneous origin of the pegmatite, followed by moderate metamorphic reheating some time after emplacement and cooling.

Conclusions

Petrographic evidence shows that the Gloserheia pegmatite was subjected to some post-crystallization alteration. The Rb-Sr data for the micas and plagioclase indicate that this alteration occurred well after emplacement of the pegmatite, possibly at the time given by the 860–874 Ma K-Ar biotite dates of O'Nions et al. (1969), Neumann (1960) and Broch (1964) in the Bamble Sector. The pegmatite minerals were open chemical systems only in small part since the $\delta^{18}O$-values are within the range of normal granite pegmatite values, and the relative order of $\delta^{18}O$-values for the minerals also is normal. The weak secondary metamorphism caused sericitization of the plagioclase and a gain in radiogenic Sr, but did not reset the Rb-Sr system in the relatively unaltered potassic feldspars, which yield a Rb-Sr date of 1062 ± 11 Ma (M.S.W.D. = 90) and an initial 87/86 ratio of 0.7023 ± 0.0002. The feldspars also give a Pb-Pb isochron age of 1085 ± 28 Ma for the least-radiogenic leads. These dates compare favorably with the best value for the age of initial crystallization of the pegmatite: the U-Pb concordia intersection age of 1060^{+8}_{-6} Ma on euxenite.

If the second stage $\mu(^{238}U/^{204}Pb)$of 9.74 in the Stacey & Kramer's (1975) two stage lead evolution model is adjusted to 9.695, the feldspar lead line in Figure 8 becomes a single stage lead line. This small difference in μ indicates that the source of original lead in the Gloserheia pegmatite is essentially the same as that for the conformable lead deposits used to construct the model. Also, the initial ratio of 0.7023 ± 0.0002 for the potassium feldspar isochron (Figure 4) is in the range for a 'mantle' igneous source of magma for the pegmatite. Remelted crustal material does not appear to contribute to the source of the Gloserheia pegmatite magma.

The geochronological data on this post-tectonic pegmatite limit the last major metamorphism in the area to >1060 Ma. The pegmatite was derived from a mantle source. It may represent either an early stage of the episode of crustal generation that culminated in the intrusion of abundant granites in the 1000–900 Ma period, or the last stage of a tectonothermal episode that waned ~1200 Ma ago, in the Bamble Sector.

Acknowledgements. – The isotopic analyses were carried out in the University of Alberta laboratories, whose operations are strongly supported by NSERC operating grant A-1168 to H.B. Mr. L.W. Day, Mr. D. Krstic and Mr. A. Stelmach gave technical support, and the Rb-mass spectrometer was maintained under the direction of Dr. G. L. Cumming. John Brommeland deserves special thanks for his careful sampling of the pegmatite, as does T. V. Segalstad for his comments on the stable-isotope data.

Manuscript received November 1983

References

Aldrich, L. T., Wetherill, G. W., Tilton, G. R. & Davis, G. L. 1956: The half-life of ^{87}Rb. *Physical Review 104,* 1045–1047.

Åmli, R. 1975: Mineralogy and rare earth geochemistry of apatite and xenotime from Gloserheia granite pegmatite, Froland, southern Norway. *Am. Mineral. 60,* 607–620.

Åmli, R. 1977: Internal structure and mineralogy of the Gloserheia granite pegmatite, Froland, southern Norway. *Nor. Geol. Tidsskr. 57,* 243–262.

Baadsgaard, H. & van Breemen, O. 1970: Thermally-induced migration of Rb and Sr in an adamellite. *Eclogae geol. Helv. 63/1,* 31–44.

Broch, A. O. 1964: Age determination of Norwegian minerals up to March, 1964. *Nor. geol. unders. 228,* 84–113.

Brooks, C. 1968: Relationship between feldspar alteration and the precise postcrystallization movement of rubidium and strontium isotopes in a granite. *Jour. of geophys. Res. 73,* 4751–4757.

Chaplin, C. E. 1981: *Isotope geology of the Gloserheia granite pegmatite, south Norway.* Unpubl. M. Sc. Thesis, Univ. of Alberta.

Clayton, R. N. 1981: Isotopic Thermometry. pp. 85–109 in: *Advances in Physical Geochemistry, Vol. 1. Thermodynamics and Melts.* Newton, R., Narrotsky, L. & Wood, B. (Eds.). Springer-Verlag, New York.

Clayton, R. N., & Mayeda, T. K. 1963: The use of bromine pentafluoride in the extraction of oxygen from oxides and silicates for isotopic analysis. *Geochim. Cosmochim. Acta. 27,* 43–52.

Craig, H. 1961: Standards for reporting concentrations of deuterium and oxygen-18 in natural waters. *Science 133,* 1833–1834.

Falkum, T. & Pedersen, J. S. 1980: The Sveconorwegian orogenic belt, a case of late-Proterozoic plate-collision. *Geol. Rundschau 69,* 622–647.

Field, D. & Råheim, A. 1979: Rb-Sr total rock isotope studies on Precambrian charnockitic gneisses from south Norway: Evidence for isochron resetting during a low-grade metamorphic deformational event. *Earth and Planet. Sci. Lett. 45,* 32–44.

Jacobsen, S. & Heier, K. S. 1978: Rb-Sr systematics in metamorphic rocks, Kongsberg sector, S. Norway. *Lithos 11,* 257–276.

Killeen, P. G. & Heier, K. S. 1975: Radioelement distribution and heat production in Precambrian granitic rocks, S. Norway. *Vid. Akad. Skr. I, Mat.-Nat. Kl., Nye serie 35.*

Krogh, T. E. 1973: A low-contamination method for hydrothermal decomposition of zircon and extraction of U and Pb for isotopic age determinations. *Geochim. Cosmochim. Acta 37,* 485–494.

Ludwig, K. R. 1980: Calculation of uncertainties of U-Pb isotope data. *Earth Plan. Sci. Lett. 46,* 212–220.

Ludwig, K. R & Silver, L. T. 1977: Lead-isotope inhomogeneity in Precambrian ingneous K-feldspars. *Geochim. Cosmochim. Acta 41,* 1457–1471.

Neumann, H. 1960: Apparent ages of Norwegian minerals and rocks. *Nor. Geol. Tidsskr. 40,* 173–189.

O'Nions, R. K. & Baadsgaard, H. 1971: A radiometric study of polymetamorphism in the Bamble region, Norway. *Contr. Mineral. Petrol. 34,* 1–21.

O'Nions, R. K., Morton, R. D. & Baadsgaard, H. 1969: Potassium-argon ages from the Bamble sector of the Fennoscandian shield in south Norway. *Nor. Geol. Tidsskr. 49,* 171–190.

Pedersen, S., Berthelsen, A., Falkum, T., Graversen, O., Hageskov, B., Maaløe, S., Petersen, J. S., Skjernaa, L. & Wilson, J. R. 1978: Rb/Sr dating of the plutonic and tectonic evolution of the Sveconorwegian province, S. Norway. *In* R. E. Zartman (Ed.), *Short Pap. 4th I.C.G.C.I.G.,* U.S. Geol. Surv., Open-File Rep. 78, 329-331.

Smalley, P. C., Field, D. & Råheim, A. 1983: Resetting of Rb-Sr whole rock isochrons during Sveconorwegian low-grade events in the Gjerstad augen gneiss, Telemark, southern Norway. *Isotope Geoscience 1,* 269–282.

Stacey, J. S. & Kramers, J. D. 1975: Approximation of terrestrial lead evolution by a two-stage model. *Earth Planet. Sci. Lett. 26,* 207–221.

Taylor, B. E. & Friedrichsen, H. 1978: Stable isotope studies of granitic pegmatites. *In* R. E. Zartman (Ed.), *Short Pap. 4th I.C.G.C.I.G.,* U.S. Geol. Surv., Open-File Rep. 78, 422–423.

Taylor, B. E. & Friedrichsen, H. 1983: Light stable isotope systematics of granite pegmatites from North America and Norway. *Isotope Geoscience 1,* 127–167.

Torske, T. 1977: The South Norway Precambrian region – a Proterozoic Cordillerantype orogenic segment. *Nor. Geol. Tidsskr. 57,* 97–120.

Wasserburg, G. J. 1963: Diffusion processes in lead-uranium systems. *J. Geophys. Res. 68,* 4823–4846.

Wetherill, G. W. Wasserburg, G. J., Aldrich, L. T. & Tilton, G. R. 1956: Decay constants of K^{40} as determined by the radiogenic argon content of potassium minerals. *The Phys. Review 103,* No. 4, 987–989.